

# Simulation and prediction of river morphologic changes using RubarBE

K. EL Kadi Abderrezzak

*Hydrology and Hydraulics Research Unit, Cemagref, Lyon, France*

A. Paquier

*Hydrology and Hydraulics Research Unit, Cemagref, Lyon, France*

**ABSTRACT:** RubarBE is a one-dimensional model for routing water and sediment transport through fixed or movable bed channels. The code simulates and predicts changes in bed composition, channel profile and cross-sectional geometry. This paper provides a general description of the concepts, approaches and hypothesis used in this model. A series of numerical simulations of sediment transport is described in this paper, with the objective of testing the performance and the potential application of RubarBE. The results of the simulations are analysed and discussed. Cross-comparison of different parameters of the model (deposition and scour rate, sediment transport, bed and water profiles...) allows some validation of the system of equations and hypothesis of our modelling system and provides some keys and ideas for further development of the code.

## 1 INTRODUCTION

Sediment transport and river morphology studies have gained increasing importance in recent years due to environmental concerns and the need to develop engineering and management strategies for sustainable use of water resources and associated infrastructures (Yang 2000). Evaluating the transport, erosion and deposition of sediments is a key element for describing and understanding the behaviour of rivers. Given that, considerable research effort has been put into the simulation of sediment transport and morphology change in rivers. A lot of computer programs have been developed in the last decades. These models provide numerical solutions for complicated situations that include movable bed and sediment transport. Most of the codes that were developed in the past decades, like HEC6 (Thomas & Prashum 1977), IALLUVIAL (Karim & Kennedy 1982) and SEDICOUP (Holly & Rahuel 1990), were built on a one-dimensional approach.

RubarBE described here is a one-dimensional flow and sediment transport model that has been developed by Cemagref in order to solve as simply as possible the requirements of engineers about river problems.

This paper is organised as follows. First, a general description of the concepts and approaches used in RubarBE is provided. Then, several applications of the model are presented to illustrate its capabili-

ties and range of applications. First, the model is tested on problems with theoretical solutions and on laboratory experiments, and then applied to field problems. The results of the numerical simulations are analysed and discussed.

## 2 DESCRIPTION OF RUBARBE

One-dimensional sediment transport models tend to be easier to parameterise and require fewer assumptions about sediment transport processes than two- and three-dimensional models (Candfield et al. 2002). The Hydrology and Hydraulics Research Unit of Cemagref has developed a 1-D model, RubarBE, for predicting variation of longitudinal bed profile along rivers and changes in the cross-sectional geometry. This computer model has two components: a component to simulate the flow and a component to characterise the changes in river morphology due to erosion or deposition of sediment.

Classical one-dimensional models that represent sediments only by a mean diameter  $D_{50}$  clearly do not fully describe the processes that occur in many channels such as armouring. Therefore, RubarBE represents sediments by a mean diameter  $D_{50}$  and a complementary parameter, the standard deviation  $S$ . The standard deviation is assessed as the square root

of the ratio between  $D_{84}$  and  $D_{16}$   $\left( \sqrt{\frac{D_{84}}{D_{16}}} \right)$ . It was

selected as it appears convenient to describe grain size distribution in a river for which sediments are homogeneous (Shih & Komar 1990).

RubarBE includes features such as:

- Computing unsteady flow in open channels with both fixed and movable bed and dealing with sub critical and super critical flow regimes.
- Taking in account the space lag effects by introducing a specific equation.
- Introducing various empirical relationships for calculating the sediment transport capacity in order to adapt the modelling to the characteristics of the application.
- Incorporating empirical relations to describe the mixtures of sediments that occur during the various calculation steps.
- Computing the distribution of boundary shear stress in a cross-section by using the Merged Perpendicular Method (Khodashenas 1998, Khodashenas & Paquier 1999).
- Computing the distribution of boundary critical shear stress in a cross-section by a relation from (Ikeda 1982).
- Simulating both the changes of riverbed composition and of cross-sectional geometry using the previous components of the code.

Data requirements for this model are modest, involving only a few parameters. Thus, the model is relatively easy to calibrate and to implement.

## 2.1 Mathematical basic model

RubarBE model relies on:

### De Saint Venant equations for water.

**Continuity equation for sediments** written as follows:

$$(1-p) \frac{\partial A_s}{\partial t} + \frac{\partial Q_s}{\partial x} = q_s \quad (1)$$

where  $A_s$  is bed-material area ( $m^2$ ),  $Q_s$  is sediment discharge ( $m^3/s$ ),  $q_s$  is lateral sediment flow per unit of length ( $m^2/s$ ) and  $p$  porosity.

These equations are completed by a **sediment transport capacity formula**; for instance, the (Meyer-Peter & Müller 1948) formula for bedload has been used for the applications here below:

$$C_s = \frac{8L_a \sqrt{g}}{(\rho_s - \rho) \sqrt{\rho}} \left( \rho J R - \theta_c D_{50} (\rho_s - \rho) \right)^{3/2} \quad (2)$$

where  $C_s$  is sediment transport capacity ( $m^3/s$ ),  $\theta_c$  is dimensionless critical stress,  $D_{50}$  is median diameter of sediment (m),  $J$  is friction slope,  $L_a$  is the active width (m) i.e. the width in which sediment transport is effective,  $\rho_s$  is density of sediment ( $kg/m^3$ ),  $\rho$  is density of water ( $kg/m^3$ ).

Finally, a **space lag equation** can be added to introduce a difference between the sediment transport capacity and the actual transport rate that may differ if geometry is not uniform. In RubarBE, the actual sediment transport rate  $Q_s$  is linked to the sediment transport capacity  $C_s$  through the following relation:

$$\frac{\partial Q_s}{\partial x} = \frac{C_s - Q_s}{D_{char}} \quad (3)$$

where  $D_{char}$  is the lag distance (m).

De Saint Venant equations are solved by a second-order Godunov-type explicit scheme (Paquier 1995). If the parameters in the sediment transport function for a cross-section can be assumed to remain constant during a time step, we can suppose that there is a little variation of the cross-sectional geometry (Yang & Simoes 1998). Thereby, sediment routing (equation 1) can be uncoupled from the water surface profile computations. In practice, this condition can be met by using a small enough time step.

Sediment routing is accomplished by a similar finite difference method. Changes in bottom level are performed at every time step. Solving the equation (1) means estimating at every time step, the input and output of sediments for one cell and spreading the erosion or deposition volume across the cell. Values of the cross-sectional flow area  $A$  and flow discharge  $Q$  are computed at the middle of a cell between two cross-sections. Thus, it is simpler to compute  $Q_s$  also in this middle and to identify it with respectively input and output of sediments if the sediment cell is shifted by half a space step (Balayn 2001).

## 2.2 Sediment modelling system

Inside one cell, a sedimentary compartment corresponds to a set of sediments that have a coherent behaviour. We distinguish four compartments:

- A compartment  $M_{am}$  of input sediments and a compartment  $M_{av}$  of output sediments.
- A compartment  $A$  of the active layer: it contains all the sediments that have moved inside one cell during one time step. Sediment

particles are continuously exchanged between flow and the active layer.

- A compartment B of one or several substrate layers: it reflects historical deposition of sediments on the riverbed or undisturbed subsurface.

Sediment particles of each compartment are characterised by the mass  $M$ , the mean diameter  $D$  and the standard deviation  $S$ . Thus, in a cell, the sediment transfers are schematised as in Figure 1 (Balayn 2001).

When sediment particles pass across a cell, they either reach the downstream of the cell, or settle on the active layer. Entrainment of sediment particles from the active layer and its exchanging with flow causes particles travelling from upstream to be mixed with those from the active layer.

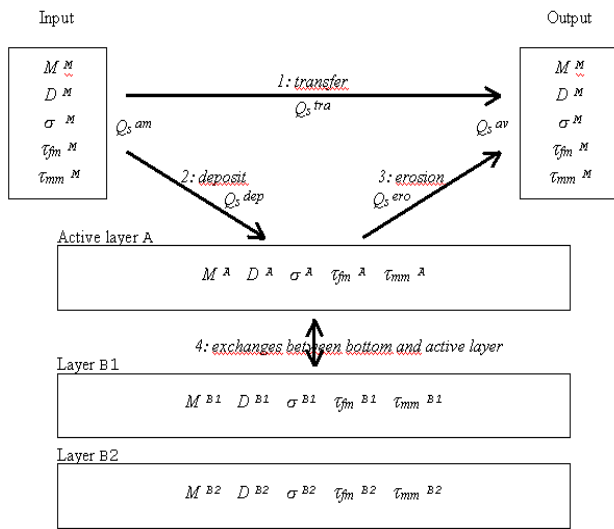


Figure 1. Representation of the sharing of sediments inside one cell (Balayn 2001)

$\tau_{fm}$  is the shear stress below which transported sediment particles begin to deposit.  $\tau_{mm}$  is the shear stress above which sediment particles begin to move.

The mass of the active layer depends on the sediment discharge, the sediment velocities and the dimension of the cell. The model assumes that this mass is defined by  $C_s * \Delta x / U$ , where  $C_s$  is the sediment transport capacity,  $\Delta x$  is the space step and  $U$  the mean water velocity.

The characteristics of the sediments resulting from the mixing or the sharing of two compartments are defined in the model by empirical relations (Balayn 2001).

### 2.3 Computation of cross-section deformation

RubarBE computes the deformation of cross-sections is computed with the assumption that scour and deposition are directly related to shear stress. The distribution of boundary shear stress around the wetted perimeter of an open channel is governed by cross-sectional geometry, roughness distribution and the existence of secondary flows. Precise computation of shear stress distribution is extremely difficult in one-dimensional models. Thus, empirical methods constitute a good alternative.

RubarBE can calculate the boundary shear distribution  $\tau_j$  in a cross-section in two ways: either from the uniform equation using water volumetric density  $\rho$ , gravity acceleration  $g$ , hydraulic radius  $R$  and energy slope  $J$  ( $\tau_j = \rho g R J$ ,  $R$  is computed on the base of the total area and perimeter of the flow) or from the Merged Perpendicular Method. The first method assumes that the boundary shear stress is constant around the wetted perimeter. The second one is a geometrical method that assumes that the energy gradient is the same in all the sub areas. More precisely, it shares the wetted area in small sub areas using the lines perpendicular to the bottom following a complex procedure described in (Khodashenas 1998, Khodashenas & Paquier 1999).

RubarBE can calculate the boundary critical shear distribution  $\tau_{cj}$  in a cross-section by a relation from (Ikeda 1982):

$$\tau_{cj} = K \tau_{cj}^* \quad (4)$$

$$K = \frac{-\alpha \tan^2 \Phi \cos \beta_j + (\tan^2 \Phi \cos^2 \beta_j + \alpha^2 \tan^2 \Phi \sin^2 \beta_j - \sin^2 \beta_j)^{0.5}}{(1 - \alpha \tan \Phi) \tan \Phi} \quad (5)$$

where  $\tau_{cj}$  critical shear stress in point  $j$  of the cross-section with slope  $\beta_j$ ,  $\tau_{cj}^*$  critical shear stress in point  $j$  for horizontal bottom ( $\beta_j = 0^\circ$ ) (which may vary from one point to another one, considering, for instance, the riverbed material),  $\beta_j$  local side slope of cross-section in point  $j$ ,  $\alpha = F_L / F_D$ ,  $F_L$  and  $F_D$  are respectively dimensionless lift and drag forces,  $\phi$  angle of internal friction of sediment. For the tests here below, the following value is selected  $\alpha = 0.85$ ;  $\tau_{cj}^*$  is calculated by the Shields curve.

The mass of sediment eroded or deposited in one cross-section obtained by the computation is distributed along the section. RubarBE incorporates various empirical relationships between deformation and shear stress. In the case of erosion, the deformation  $\Delta Z_j$  of an erodible point  $j$  of one cross-section is assumed to be proportional to  $(\tau_j - \tau_{cj})^{1.5}$ . In the case of sedimentation, deposited sediment in one cross-section can be distributed in three ways:

- The cross-section is adjusted in horizontal layers.
- The entire wetted cross-section is moved uniformly up.
- The deformation  $\Delta Z_j$  of a “deposit” point  $j$  is assumed to be proportional to  $(1/\tau_j)$ .

### 3 APPLICATION CASES AND RESULTS

#### 3.1 Theoretical cases

##### 3.1.1 Knickpoint migration

Knickpoint are points of sudden change or inflection in the longitudinal profile of a stream. In general knickpoint may migrate upstream along the channel and have undesirable effects, such as causing banks collapse and undermining bridge piers. Thus, knickpoint development and propagation is a very interesting phenomenon to study.

The simulated channel has a rectangular section, 300 m long  $\times$  10 m wide by 4 m deep. The knickpoint is represented by a backward-facing step in the bed with a slope of 0.01 m/m. The upstream and downstream reaches have a slope of 0.001 m/m. The bed material and sediment feed are composed of the same coarse sand and channel width is constant. Table 1 shows the main characteristics of the simulation.

Table 1. Characteristics of the simulation

Water discharge $Q$	Manning coefficient $K$	Sediment Diameter $D_{50}$	Standard deviation $S$	Sediment feed rate $Q_s$
$m^3/s$	$m^{1/3}/s$	mm		kg/s
20	30	1	2.3	17.6

The flow discharge is maintained constant. The sediment feed rate  $Q_s$  is specified as the sediment transport capacity of the upstream and downstream reaches. On the downstream side, it is assumed that the flow acted like uniform outflow.

The porosity  $p$  of the bed material is assumed to equal to 40 %, the sediment density  $\rho_s$  to equal to  $2600 \text{ kg/m}^3$  and the angle of internal friction of sediment  $\phi$  to equal to  $30^\circ$ .

The central riverbed will suffer from degradation. Theoretically, in dynamic equilibrium, the slopes of the three parts of the channel are expected to equal to 0.001 m/m.

The simulation is accomplished with a uniformly spaced mesh, using cross-sections spaced 10 m apart. The lag distance  $D_{char}$  is assumed to equal to 1

m. The initial condition for sediment transport is  $Q_s=17.6 \text{ kg/s}$ . The distribution of the boundary shear stress is calculated by  $\tau=\rho g R J$ . The dimensionless shear stress  $\theta_c$  is assumed to be equal to 0.047.

Figure 2 shows the initial bed with the equilibrium bed and the water surface profile. The channel is in dynamic equilibrium 280 hours after the start of the simulation. RubarBE was able to predict well the scour depths and the final equilibrium slope (0.001 m/m). There is an overall close agreement between the theoretical solution (a constant riverbed slope of 0.001m/m) and the result of the simulation.

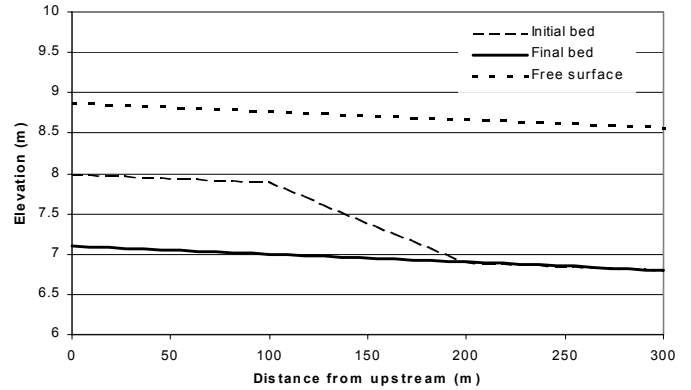


Figure 2. Initial bed, computed equilibrium bed and water surface

##### 3.1.2 Irregular straight open channel

Usually, natural channels are characterised by an irregular cross-section. An irregular straight open channel of uniform cross section (Fig. 3) is selected to validate the performance of the code. The simulated channel is 1000 m long and the channel bed slope is 0.0001 m/m.

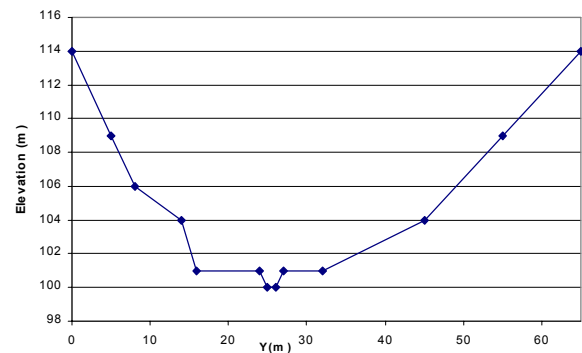


Figure 3. Channel cross-section

The bed material and sediment feed are composed of the same coarse sand. Table 2 shows the main characteristics of the simulation.

Table 2. Characteristics of the simulation

Water discharge $Q$	Manning coefficient $K$	Sediment Diameter $D_{50}$	Standard deviation $S$	Sediment feed rate $Q_s$
$m^3/s$	$m^{1/3}/s$	mm		kg/s
300	45	1	2.3	29

The flow discharge is maintained constant. The sediment feed rate  $Q_s$  corresponds to the sediment transport capacity of the simulated channel. The downstream water level is fixed at a constant value of 108.066 m.

The porosity  $p$  of the bed material is assumed to equal to 40 %, the sediment density  $\rho_s$  to equal to  $2600 \text{ kg/m}^3$  and the angle of internal friction of sediment  $\phi$  to equal to  $35^\circ$ .

For this application, a constant space step  $\Delta x$  of 100 m is used. The lag distance  $D_{char}$  is assumed to equal to 50 m. The initial condition for sediment transport is  $Q_s = 14.5 \text{ kg/s}$ . The distribution of the boundary shear stress is by the Merged Perpendicular Method. The dimensionless shear stress  $\theta_c$  is assumed to equal to 0.047. The deformation  $\Delta Z_j$  of a “deposit” point  $j$  is assumed to be proportional to  $(1/\tau_j)$ .

Figure 4 shows the initial bed as well as the channel bed profiles at different times. The channel is in dynamic equilibrium 200 days after the start of the simulation. RubarBE is able to predict both the deposition heights and the advance of the deposition front. However, the numerical results show an “inflection” in the longitudinal profile located at  $x = 910.9 \text{ m}$ . This slight change in the bed profile could be due to the influence of the downstream boundary condition and the distribution of shear stress at  $x = 910.9 \text{ m}$ . The channel bed slope upstream from the “inflection point” is about  $0.000175 \text{ m/m}$ .

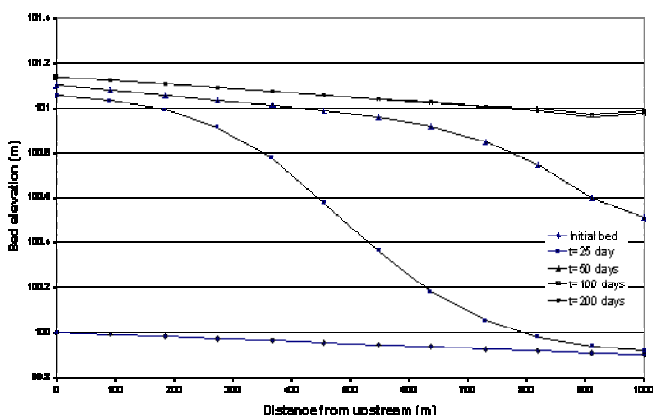


Figure 4. Initial bed and computed channel bed profiles at different times

Figure 5 shows the evolution of the cross-section at  $x = 1000 \text{ m}$ . In a concave angle of a cross-section, computed shear stress by the Merged Perpendicular Method is lower than in a convex angle. Thus high deposition is observed in the concave angles of the channel

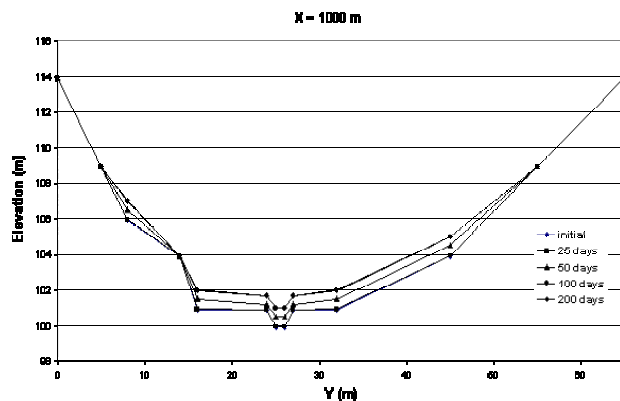


Figure 5. cross-section deformation: a)  $x = 0 \text{ m}$ , b)  $x = 1000 \text{ m}$

The evolution of the riverbed profile and the cross-sectional geometry is affected by the methods used to compute the boundary shear stress. A numerical simulation is performed with the assumptions that the shear stress distribution is calculated by  $\tau = \rho g R J$  and the boundary critical shear distribution computed from the Shields curve (the (Ikeda 1982) relation is not used).

SIM-1 refers to the simulation with the Merged Perpendicular Method and (Ikeda 1982) relation; SIM-2 refers to the simulation with  $\tau = \rho g R J$  and *critical* shear distribution from the Shields curve. Figure 6 shows the dynamic equilibrium beds resulting from the simulation SIM-1 and SIM-2. SIM-2 shows less deposition in the channel bed; the difference between SIM-1 and SIM-2 is about 0.15 m. The equilibrium bed profile computed by SIM-2 is not affected by the boundary condition: a constant slope of  $0.000175 \text{ m/m}$  is obtained through the channel bed.

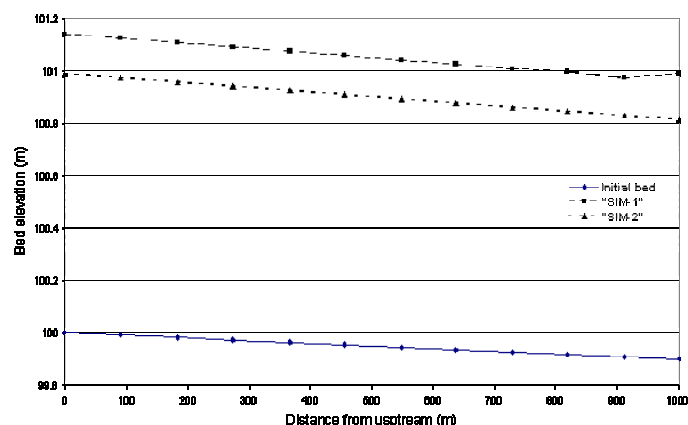


Figure 6. Initial bed, computed equilibrium bed

### 3.2 Laboratory experiment

While theoretical cases deal with long-term behaviour, the selected test case provides testing of very unsteady flow during a short period.

This test case concerns an experimental small-scale laboratory dam-break waves over movable

beds. The experiment was performed by (Spinewine 2002) in the framework of the EC-funded IMPACT project at the Department of Civil and Environmental Engineering, Université Catholique de Louvain, Belgium. The objective is to investigate the geomorphic impacts induced by very rapid and transient floods such as those resulting from dam-breaks.

An idealised dam-break problem is considered (Fig. 7). A horizontal flume of rectangular cross-sectional geometry is used. The flume has the following dimensions: length = 2.5 m, width = 0.10 m and sidewall height = 0.35 m. The reservoir is assumed to be long and has the following dimensions: length = 10 m, width = 0.10 m and sidewall height = 0.35 m. Particles composing the bed are uniform in size.

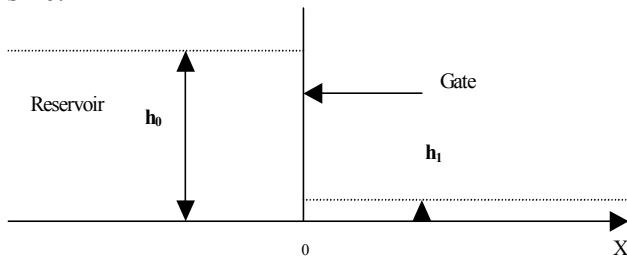


Figure 7. Idealized dam-break problem,  $h_0$  and  $h_1$  are the initial depths upstream and downstream of the dam before failure.

The sediment diameter is  $D_{50} = 3.5$  mm and the standard deviation is  $\sigma = 1$ . The porosity  $p$  of the bed material is assumed to 36 %, the sediment density  $\rho_s$  to  $1540 \text{ kg/m}^3$  and the angle of internal friction of sediment  $\phi$  to  $25^\circ$ .

The Strickler coefficient  $K$  was derived from the particle diameter through the classical Meyer-Peter and Müller formula:  $K = \frac{21.1}{D^{1/6}} = 54 \text{ (m}^{1/3}/\text{s)}$ .

Tests consisted in the sudden opening of a vertical gate that separated the initial water and sediments levels upstream and downstream of the gate. Due to highly unsteady nature of dam break flood propagation; the flume and the reservoir were described through a dense grid of cross-sections. Two constant space steps are used:  $\Delta x = 5$  cm and  $\Delta x = 20$  cm. A smaller space step allows obtaining the arrival of the flood wave in a more accurate way. A larger space step allows describing the transition between super and sub critical flow (hydraulic jump) more conveniently.

The origin of the horizontal axis is located at the gate position. The initial conditions for this case are  $h_0 = 0.10$  m if  $x < 0$  and  $h_1 = 0$  m if  $x \geq 0$ , where  $x$  is the distance along the flume. The total time of the simulation is 2 second. The initial condition for sediment transport is  $Q_s = 0 \text{ kg/s}$ .

On the upstream side ( $x = -10$  m), a constant depth of water  $h = 0.10$  m is imposed. On the downstream side ( $x = 2.5$  m), it is assumed that the flow acted like critical outflow. The upstream sediment condition is  $Q_s = 0 \text{ kg/s}$ . The time step is variable, but it is chosen so that the maximum Courant number of every cell does not exceed a limited value imposed by the model. The simulations were run for two values of maximum Courant numbers (noted  $CFL$ ): 0.5 and 0.1.

For this test case, the distribution of the boundary shear stress is calculated by  $\tau = \rho g R J$ ; the dimensionless shear stress  $\theta_c$  is calculated by the Shields curve.

For all the runs, the results show that in the near field, rapid and intense erosion accompanies the development of the dam-break wave. In the far field, the solid transport remains intense but the dynamic role of the sediments decreases (Figs. 8-9). The flow loses its capacity, the transported material is deposited.

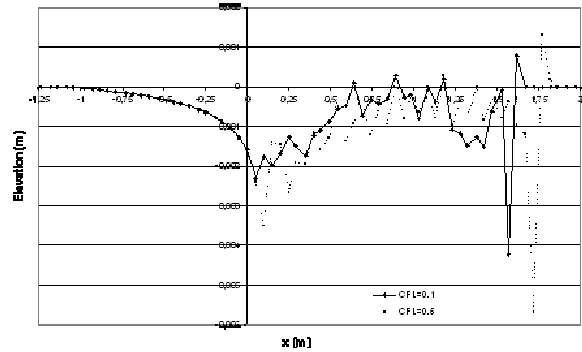


Figure 8. Bottom level:  $\Delta x = 5$  cm,  $D_{char} = 1$  m,  $t = 2$  s

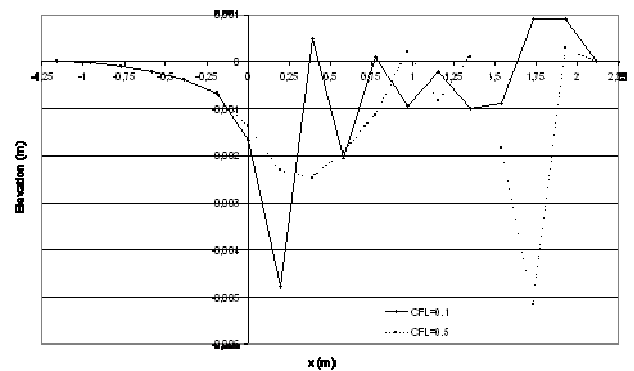


Figure 9. Bottom level:  $\Delta x = 20$  cm,  $D_{char} = 1$  m,  $t = 2$  s

Instabilities of calculations were observed during the numerical tests. Results of simulations depend on the grid spacing, the  $CFL$  (Figs. 8-9) and  $D_{char}$  values (Fig. 10). Instabilities are more marked in the case of  $CFL = 0.1$ . The difference of accuracy between the numerical results increases in the far field (Fig. 11).

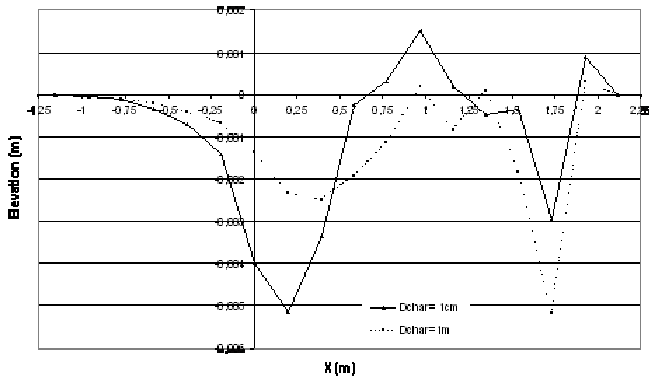


Figure 10. Bottom level evolution with spatial lag  $D_{char}$ :  $\Delta x = 20$  cm,  $CFL = 0.5$ ,  $t = 2$  s

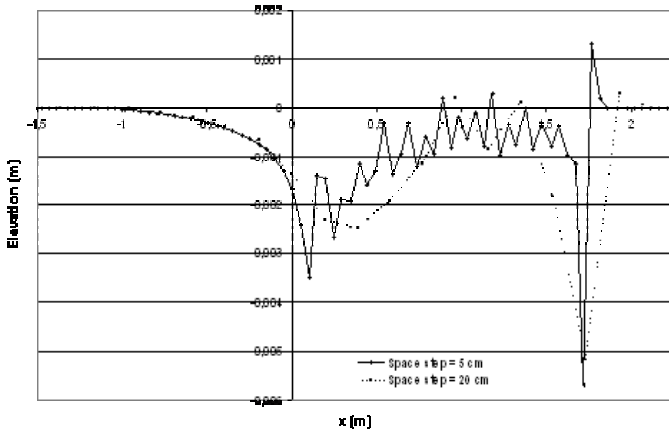


Figure 11. Bottom level evolution:  $D_{char} = 1$  m,  $CFL = 0.5$ ,  $t = 2$  s

The numerical simulations take in account only the bedload transport. This assumption may be restrictive in the modelling of flood or dam break events, where suspended load is important. Added numerical tests were carried out, in which the dimensionless critical shear stress  $\theta_c$  was supposed nil. Similar behaviour is obtained with non-nil critical shear stress (Fig. 12).

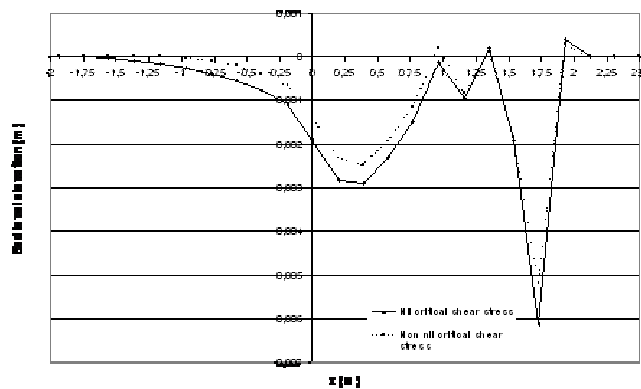


Figure 12. Bottom level evolution with nil or non nil critical shear stress:  $\Delta x = 20$  cm,  $D_{char} = 1$  m,  $CFL = 0.5$ ,  $t = 2$  s

Experimental data are compared to the numerical results. CEM-1 refers to the simulation with a space step of 20 cm,  $D_{char} = 1$  m and  $CFL = 0.5$ ; CEM-2 to the simulation with a space step of 20 cm,  $D_{char} = 1$

cm and  $CFL = 0.5$  and CEM-3 to the simulation with a space step of 5 cm,  $D_{char} = 1$  m and  $CFL = 0.5$ .

Figure 13 shows the comparison concerning the front characteristics: the time of front wave arrival is smaller with the RubarBE model. This behaviour can be explained by influence of the hypothesis and approaches used by RubarBE (average velocity, hydrostatic pressure...).

However, it must be noticed that the closest approximations to the experimental data seem to be for the numerical CEM-3, i.e. space step of 5 cm,  $D_{char} = 1$  m and  $CFL = 0.5$ . At the same cross-section the difference between the arrival times is around 0.15 s. The shape of the experimental wave front is quite similar to the numerical profiles and small grid space step provides better estimate of arrival time of the flood wave.

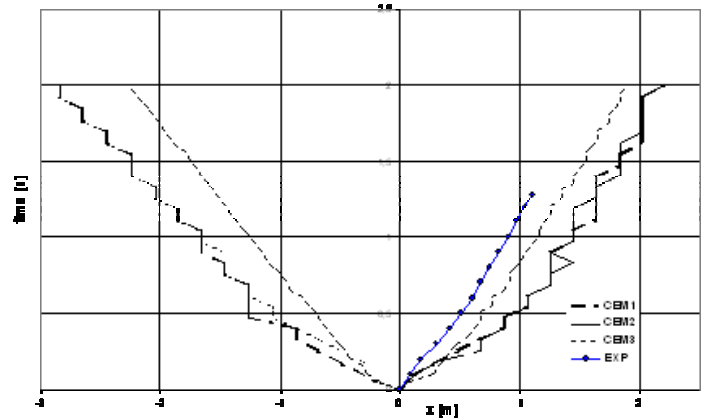


Figure 13. Front characteristics

The channel friction could affect significantly the propagation of the front wave. A Manning friction coefficient of  $0.0185 \text{ s/m}^{1/3}$ , derived from the diameter of the riverbed material, was selected. The influence of the wall friction was neglected. Then, a sensitivity analysis was carried out. Two different Manning coefficients are tested with the simulation CEM-3. Figure 14 shows that the celerity is quite dependent on the friction coefficient introduced in the numerical model. The agreement between experimental data and RubarBE simulation (CEM-3) is quite improved with a roughness of  $0.02 \text{ s/m}^{1/3}$  instead of  $0.0185 \text{ s/m}^{1/3}$  in the previous simulations.

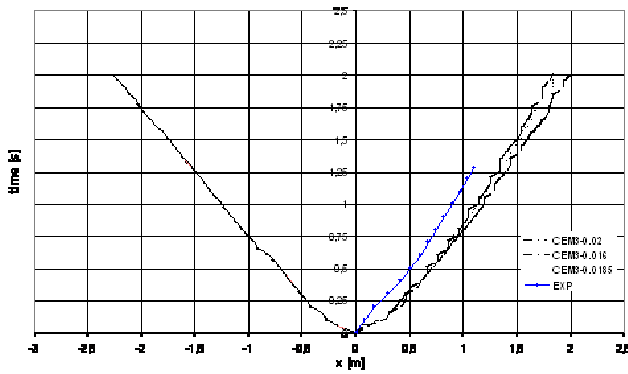
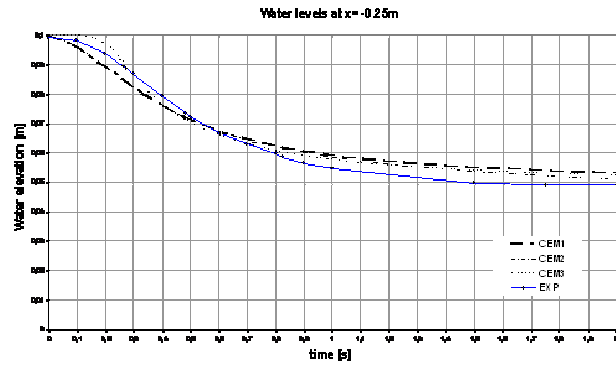
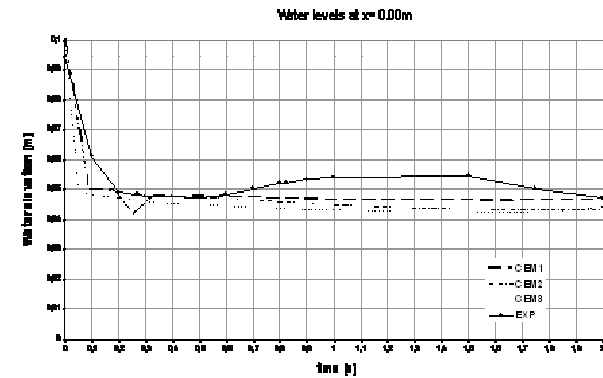


Figure 14. CEM3: front characteristics with different values of roughness

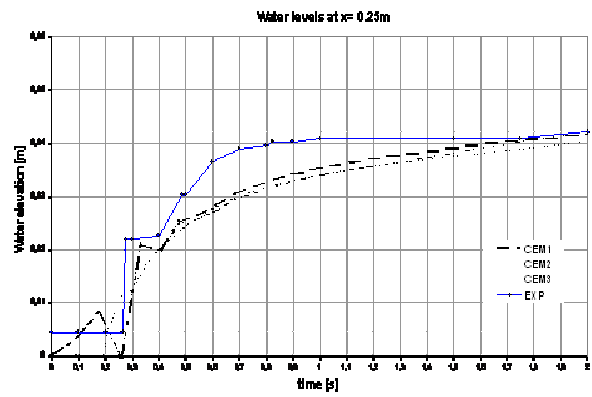
Figures 15a, b, c show the water levels evolution at three cross-sections:  $x = -0.25\text{m}$ ,  $x = 0.00\text{ m}$  and  $x=0.25\text{ m}$ . Computed water levels agree with experimental data except slight differences observed upstream from the gate. In the reservoir, the closest approximations to the experimental data seem to be for the numerical simulation CEM-3. The simulation CEM-1 provides accurate approximations to the experimental data upstream from the gate. At gate location, the water levels evolution is underestimated. Flow is critical at the gate; decoupled model is inherently less stable than the coupled model in the case of Froude numbers vary close to unity, and they may need a special treatment of time step (Cui et al. 1996)



a



b

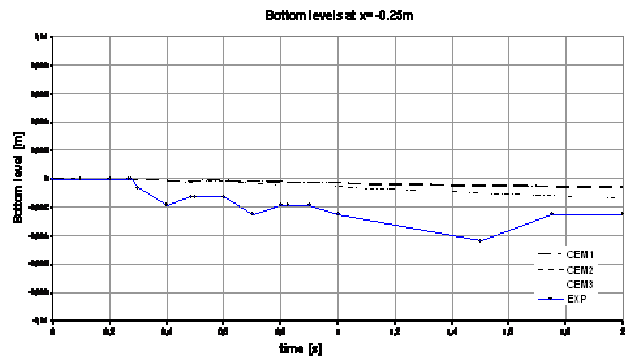


c

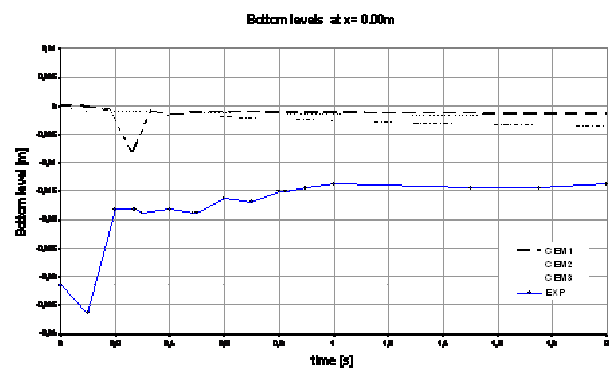
Figure 15. Water levels evolution: a:  $x = -0.25\text{ m}$ , b:  $x = 0.00\text{ m}$ , c:  $x = 0.25\text{ m}$ ,

Beyond the high concentrations of sediment that invalidate the hypothesis of one single phase (see here below), the differences between calculation and experimental results are due to the highly 3-D nature of the dam-break wave for which some of the St. Venant hypothesis (small bottom slopes and curvatures, hydrostatic pressure and uniform velocity distribution in the cross section) are certainly not verified.

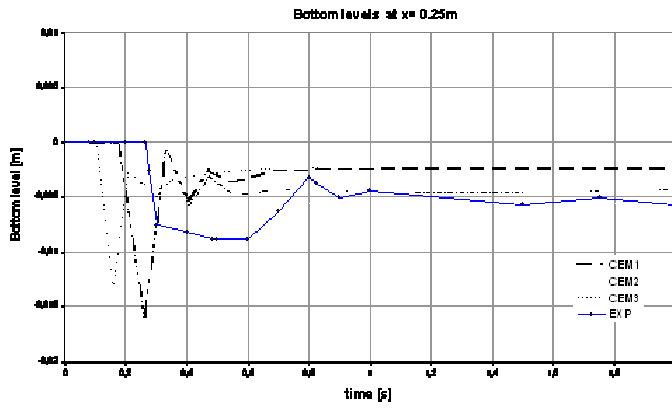
Figures 16a, b, c show the bottom position at three cross-sections:  $x = -0.25\text{ m}$ ,  $x = 0.00\text{ m}$  and  $x = 0.25\text{m}$ . Significant discrepancies between numerical and experimental results are observed through the reservoir and the channel.



a



b



c  
Figure 16. Bottom levels changes: a  $x = -0.25$  m, b  $x = 0.00$  m, c  $x = 0.25$  m

The use of the Exner equation and of a maximum sediment transport capacity does not integrate the presence of a mixture of water and sediments in high concentration. This assumption but may be restrictive in the modelling of flood or dam break events. The use of another method for calculating the sediment transport seems to be necessary to take into account high concentration transport.

### 3.2.1 3. Field application: Miribel channel

This field application consists of sediment transport and morphologic changes in the Miribel channel. This channel is located north from Lyon in France. A geomorphologic survey was carried out in the Miribel channel by (Malavoi 2000).

This case schematises the sediment transport in the channel after closing a former excavation in 1990. This pitch of about 400 000 m<sup>3</sup> is located in the upstream reach of the channel near the “Thil” village. Since sediments are trapped in this pitch, materials cannot be carried away from the upstream reach to the downstream one. As a consequence, important erosion was observed in the surrounding reaches.

The Miribel channel has a nearly rectangular section, is 16 km long and 85 m wide. The pitch is approximately 2 km long and the channel slope is about 0.00065 m/m. The bed material and sediment feed are composed of the same material. Table 3 shows the main characteristics of the simulation.

Table 3. Characteristics of the simulation

Water discharge $Q$	Manning coefficient $K$	Sediment Diameter $D_{50}$	Standard deviation $S$	Sediment feed rate $Q_s$
m <sup>3</sup> /s	m <sup>1/3</sup> /s	mm		kg/s
850	26	25	2.3	144.7

The flow discharge  $Q$  is maintained constant for a period of 20 days. The sediment feed rate  $Q_s$  is specified as the sediment transport capacity of the upstream and downstream reaches. On the downstream side, it was assumed that the flow acted like uniform outflow.

The porosity  $p$  of the bed material is assumed to equal to 30 %, the sediment density  $\rho_s$  to equal to 2650 kg/m<sup>3</sup> and the angle of internal friction of sediment  $\phi$  to be 35°.

The channel is described through a grid of cross-sections: a constant grid spacing  $\Delta x = 100$  m is used. The lag distance  $D_{char}$  is assumed to equal to 1 m. The initial condition for sediment transport is  $Q_s = 144.7$  kg/s. The distribution of the boundary shear stress is calculated by  $\tau = \rho g R J$ . The dimensionless shear stress  $\theta_c$  is assumed to 0.047. In the case of sedimentation, deposited sediment in one cross-section is distributed in horizontal layers across the channel width.

Figure 17 shows the evolution of the bed profile and free surface with time. The model predicts the progression of scour as well as deposition in the excavation. The evolution of the Miribel bed is controlled by the deposition of sediments in the pitch. The natural passage of sediments through the channel is interrupted by the pitch: sediments are washed into the excavation causing the bed upstream to erode. Downstream of the excavation the bed is lowered as the flow picks up energy on leaving the hole. At the end of the simulation, the deposition rate in the pitch is about 3 m.

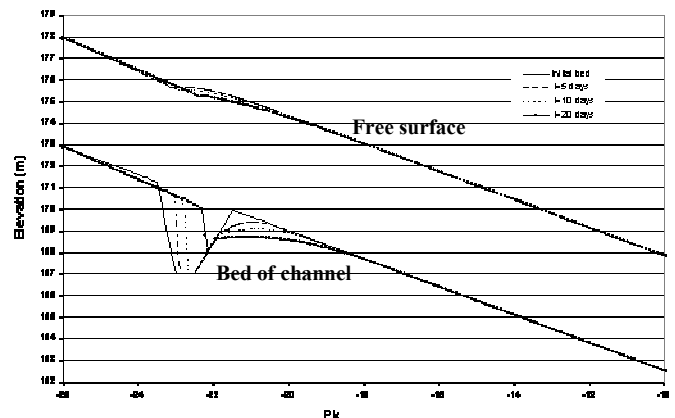


Figure 17. Miribel channel: initial bed, computed equilibrium bed and water surface.

## 4 CONCLUSIONS

RubarBE is designed to simulate single flood event and long-term scour and/or deposition. RubarBE assumes that equilibrium conditions are not necessary reached within each time step; the in-

fluence of unsteady conditions during flood events is taken in account through a loading equation.

This paper shows some examples of applications. The model can be used for applications to engineering problems, such as knickpoint migration. In the case of dam-break waves, the use of the Exner equation and of a maximum sediment transport capacity does not integrate the presence of a mixture of water and sediments in high concentration. This assumption is valid for long-term simulations of bed aggradation or degradation, but may be restrictive in the modelling of flood or dam break events. The use of other methods for calculating the sediment transport seems to be necessary to take into account high concentration transport.

RubarBE is in stage of continuous development and improvement. A decisive step was to integrate the calculation of the distribution of the shear stress in the transversal direction and various relationships between deformation and shear stress (Paquier & Khodashenas 2002). Next step should be the validation of the modelling of graded sediment. However, there is still no provision for simulating the development of meanders and the effect of bed forms.

## 5 ACKNOWLEDGEMENTS

The authors wish to acknowledge the financial support offered by the European Commission for the IMPACT project under the fifth framework programme (1998-2002), Environment and Sustainable Development thematic programme.

## 6 REFERENCES

- Balayn, P. 2001. *Contribution à la modélisation numérique de l'évolution morphologique des cours d'eau aménagés lors de crues*. PhD Thesis. Lyon : Université Claude Bernard Lyon 1.
- Candfield, H.F., Wilson, C. J., Reneau, S. L., Thomas, W. A., Lane, L. J., Wetherbee, G. A. & Crowell, K. J. 2002. Calibration of a one-dimensional sediment transport model on a two-dimensional scour problem. Meeting. Groundwater and Surface Water Hydrology (Posters). The Geological Society of America, 98th Annual Meeting; Corvallis, 13-15 May.
- Cui, Y., Parker, G. & Paola, C. 1996. Numerical simulation of aggradation and downstream fining. *Journal of Hydraulic Research*, Vol. 34, N° 2: 185-204.
- Engelund, F. & Hansen, E. 1967. A Monograph on Sediment Transport in Alluvial Streams. *Teknisk Forlag, Technical Press*.
- Holly, F.M. and Rahuel, J.L., 1990. New numerical/Physical framework for mobile-bed modeling, Part 1: numerical and physical principals. *Journal of Hydraulic Research*, Vol.28, N° 4: 401-416.
- Karim, M.F. & Kennedy, J.F. 1982. *IALLUVIAL: a computer based flow and sediment routing for alluvial streams and its application to the Missouri River*. Iowa: Iowa Institute of Hydraulic Research, Report N° 343.
- Khodashenas, S.R. 1998. *Modification de la topographie d'une rivière due au transport des sédiments*. PhD Thesis, Lyon: Ecole Centrale de Lyon.
- Khodashenas, S.R. & Paquier, A. 1999. A geometrical method for computing the distribution of boundary shear stress across irregular straight open channels. *Journal of Hydraulic Research*, Vol.37, N° 3: 381-388.
- Ikeda, S. 1982. Incipient motion of sand particles on sans slopes. *Journal of Hydraulic Division*, Vol.108, N° HY1: 95-114.
- Malavoi, J.R. 2000. *Etude géomorphologique du canal de Miribel*. Lyon: Hydratec-Voies navigables de France.
- Meyer-Peter, E. & Müller, R. 1948. Formulas for bed-load transport. *Report on second meeting of IARH. IAHR*, Stockholm: 39-64.
- Paquier, A. 1995. *Modélisation et simulation de la propagation de l'onde de rupture de barrage*. PhD Thesis, Saint-Etienne: Université Jean Monnet.
- Paquier, A. and Khodashenas, S.R., 2002. River bed deformation calculated from boundary shear stress. *Journal of Hydraulic Research*, 40(5): 603-609.
- Shih, S.-M. & Komar, P.D. 1990. Hydraulic controls of grain-size distributions of bedload gravels in Oak Creek, Oregon, USA. *Sedimentology*, 37: 367-376.
- Spinewine, B. & Zech, Y. 2002. Dam-break waves over movable beds: a "flat bed" test case. 2nd IMPACT Workshop (EU-funded research project on Investigation of Extreme Flood Processes and Uncertainty), Mo-i-Rana, Norway.
- Thomas, W.A. & Prashum, A.I. 1977. Mathematical model of scour and deposition. *Journal of Hydraulic Division*, Vol.110, N° 11: 1613-1641
- Yang, C.T., 2000. Sedimentation and River Morphology Studies in the Bureau of Reclamation. *4th International Conference on Hydro-Science and engineering (ICHE)*. Seoul.
- Yang, C.T., & Simos, J.M. 1998. *Sediment transport and river morphologic changes*. Denver: U.S. Bureau of Reclamation, Technical Service Center, Sedimentation and River Hydraulics Group.